

Effect of Carbon Black Loading on Fluoroelastomer–Solvent Interactions

TEJRAJ M. AMINABHAVI, SUJATA F. HARLAPUR

Department of Chemistry, Karnatak University, Dharwad, 580 003 India

Received 19 March 1997; accepted 27 October 1997

ABSTRACT: An analysis of the molecular transport of organic liquids into fluoroelastomer membranes containing varying amounts of carbon black has been undertaken by the sorption–desorption gravimetric method. The variation in carbon black loading and temperature showed a significant effect on their transport characteristics. Diffusion coefficients were calculated from Fick's equation. Experimental sorption–desorption results were analyzed in terms of concentration profiles obtained from a solution of Fick's equation as well as by a numerical method based on the finite difference technique. Arrhenius activation parameters were estimated from the temperature-dependent diffusion and permeation data. The results of this study are discussed in terms of polymer–solvent interactions. © 1998 John Wiley & Sons, Inc. *J Appl Polym Sci* 68: 815–825, 1998

Key words: fluoroelastomer; sorption; diffusion; VITONs

INTRODUCTION

In recent years, there has been a renewed interest in the study of the transport of liquids into engineering polymer membranes due to their varied applications in a number of membrane-based separation processes (MBSPs).^{1–5} For a successful application of polymer membranes in these areas, it is important to understand sorption, desorption, and diffusion of liquid molecules into the membrane materials. Liquid transport into polymer membranes has been studied by a solution–diffusion model, that is, penetrant molecules become sorbed inside the polymer matrix at one side of the membrane with the highest chemical potential and then diffuse within the matrix in the direction of a lower chemical potential. However,

polymer morphology in addition to the type and extent of additives such as those including carbon black particles influence the transport characteristics of polymer–solvent systems. The addition of carbon black while compounding the rubbery polymers increases their dimensional stability, further affecting their transport characteristics.^{6–9} However, it would be of interest to know how carbon black loading can affect their transport characteristics.

In the present study, we focused our attention on the phenomenological aspects of the sorption, desorption, and diffusion of dimethyl sulfoxide (DMSO), dimethylformamide (DMF), tetrahydrofuran (THF), 1,4-dioxane, and dimethylacetamide (DMAc) into three fluoropolymer membranes with different carbon black loadings. The polymer membranes used in the present study are DuPont's VITON A-201C series with the designated sample numbers 2093, 2094, and 2095 containing, respectively, 10, 20, and 30% by weight of carbon blacks. These polymers are known for their excellent fuel, solvent, and chemical resistivity.

Correspondence to: T. M. Aminabhavi.

Contract grant sponsor: All India Council for Technical Education, New Delhi; contract grant number: 8017/RDII/96 (ID No. 138.23).

Journal of Applied Polymer Science, Vol. 68, 815–825 (1998)
© 1998 John Wiley & Sons, Inc. CCC 0021-8995/98/050815-11

vity properties in addition to outstanding environmental stability over a wide range of temperatures. VITONs are not recommended for service in low molar mass esters and ethers, ketones, certain amines, hot anhydrous hydrofluoric or chlorosulfonic acids, and alkyl phosphate esters. This prompted us to investigate the interactions of highly aggressive organic liquids chosen with the VITONs. Deviations in transport behavior due to morphological differences of the polymers were studied by selecting polymers with different carbon black loadings. The study was performed at 25, 44, and 60°C. Thus, sorption (S), desorption (D), resorption (RS), and redesorption (RD) that is, S–D–RS–RD, properties were evaluated. From the sorption data, concentration profiles of liquids into the membrane materials were calculated using a numerical method¹⁰ and also by solving Fick's equation under suitable initial and boundary conditions.¹¹

EXPERIMENTAL

The VITON-A-type fluoroelastomers¹² are based on the copolymerization of vinylidene fluoride, $\text{CH}_2=\text{CF}_2$ (VF_2), and hexafluoropropylene,

$\text{CF}_2=\text{CF}-\text{CF}_3$ (HFP), with a general polymer structure: $-(\text{CH}_2-\text{CF}_2)_a-(\text{CF}_2-\text{CF}-\text{CF}_2)_b-$, where the subscripts a and b are the degree of polymerization of respective homopolymer. These polymers prepared by the emulsion polymerization method¹³ are primarily developed for military applications. The VF_2 monomers with a homopolymer glass transition temperature (T_g) of -40°C and HFP with a homopolymer T_g of 165°C were used to synthesize the copolymer. Here, the lower T_g of VF_2 helps to retain the elastomeric characteristics and tends to crystallize with the hydrocarbon portion of the polymer that swells in organic liquids. However, the higher T_g HFP portion breaks up crystallinity to give an elastomeric behavior. The fluorine content of the polymers is 66% and the Mooney viscosity as measured by MI 1 + 10 at 100°C is around 65 with the weight-average molar mass, \bar{M}_w , equal to 327,000.

The rubber compound formulations given in Table I were mixed in a "B" Banbury mixer using an upside-down mix procedure. All the dry ingredients were preblended before adding in the mixing chamber, but the polymer was added last. The ram was lowered and compounds were mixed for 2–2.5 min. Stocks were discharged at an indicated temperature of 93°C , but the actual stock

Table I Mix Compositions and Mechanical Properties of Fluoroelastomers

Ingredients/Properties	Samples		
	2093	2094	2095
<u>Ingredients</u>			
VITON A-201C	100	100	100
Magnalite D ^a	3	3	3
Calcium hydroxide	6	6	6
Carnauba wax ^b	1	1	1
Carbon black N990	10	20	30
<u>Properties (slab cured at 177°C for 10 min)</u>			
Mooney viscosity (ML 1 + 10, at 121°C)			
ASTM D1646-90	42	50	65
100% modulus (MPa) ^c	3.0	4.0	5.0
Tensile strength (MPa) ^c	8.8	10.8	12.6
Elongation at break (%) ^c	191	205	261
Hardness, durometer ASTM D2240-87	75	76	77
Specific gravity	1.82	1.82	1.82

^a Magnalite D is a trademark of Marine Magnesium Company. It is a high activity magnesium oxide.

^b Carnauba wax is a natural wax used for processing.

^c ASTM D412-87, pulled at 8.5 mm/s.

Table II Molar Volume (V), Viscosity (η), Dipole Moment (μ), and Solubility Parameter (δ) of Liquids at 25°C

Liquid	V (cm ³ mol ⁻¹)	η (mPa s)	μ	δ (J cm ⁻³) ^{1/2}
DMSO	71.3	1.99	4.06	24.5
DMF	77.5	0.80	3.24	24.8
THF	82.1	0.46	1.75	20.3
1,4-Dioxane	85.7	1.20	0.45	20.7
DMAc	93.1	0.93	3.71 ^a	22.1

^a At 30°C.

temperature was around 121°C. The stocks were milled on a 16-in. two-roll mill for 2 min; they were sheeted off the mill and allowed to rest overnight at 24°C before being resheeted on the mill to have the samples die cut for curing. Samples were cured for 10 min at 177°C in an electric press. On the next day, these were postcured at 232°C for 24 h. Some representative mechanical properties are also included in Table I.

Sheets of fluoroelastomers (sample designation 2093, 2094, and 2095) were fabricated at DuPont's Chemical Laboratory, Stow, Ohio, (courtesy of Mr. Bill Stahl) into 15 × 15 cm slabs with the initial thickness ranging from 0.214 to 0.245 cm. Circular disc-shaped samples with a diameter of 1.975 cm were cut from large sheets using a sharp-edged carbon-tipped steel die. The cut samples were dried in vacuum desiccators over anhydrous calcium chloride at room temperature for at least 24–72 h before the start of the sorption experiments.

Reagent-grade DMSO, DMF, THF, 1,4-dioxane, and DMAc (all from S.D. Fine Chemicals, India) were used without further purification. Some representative solvent property data are given in Table II.

S–D–RS–RD Testing

The S–D–RS–RD experiments were performed by placing the known dry weights of the cut polymer samples into specially designed screw-tight test bottles containing about 15–20 cm³ of the test liquids. At periodic intervals of time (initially, these intervals were within 2–3 min), the submerged samples were removed from the test bottles, the surface-adhered liquid drops were wiped off by slowly pressing them in between smooth filter paper wraps, weighed immediately on a digi-

tal Mettler Balance, Model AE 240 (Switzerland), within the precision of ±0.01 mg, and placed back into the test bottles. Since the time required for this operation was less than 30 s, this procedure did not introduce large errors in weight uptake data of the samples. All samples reached equilibrium sorption within 48 h, which remained constant over an extended period of 3–4 days. After completion of the sorption runs, the sorbed samples were placed in a vacuum oven for desorption measurements. The percent weight uptake or loss of the samples were calculated as explained before.^{14–16} Sorption experiments were conducted at 25, 44, and 60°C and resorption runs at 25°C were performed in the same manner as those of sorption tests. The desorption and redesorption experiments were also performed at 25°C.

Dimensional changes of the polymer samples at 25°C were monitored by measuring the changes in the thickness and diameter of the samples during swelling. The thickness (up to the accuracy of ±0.001 cm) of the samples was measured using a micrometer screw gauge (Germany), whereas increase in the lateral dimension was measured by a Vernier caliper (Toledo, Switzerland).

RESULTS AND DISCUSSION

Sorption results are expressed in weight percent units and these are calculated from the amount of liquid absorbed in g per 100 g of the polymer. For the desorption experiments, these results represent the loss in weight of the samples. Sorption data at 25, 44, and 60°C for the three polymer samples are presented in Table III. These results suggest a widely varying trend, but are not highly systematic with temperature for the majority of the liquids. For THF, in the case of the 2093 and

Table III Sorption (S), Desorption (D), Resorption (RS), and Redesorption (RD) Data in Wt % Units for the Fluoroelastomer Samples with Liquids at Different Temperatures

Liquid	S			D	25°C	
	25°C	44°C	60°C		RS	RD
2093 (10% Carbon Black)						
DMSO	71.9	83.7	84.6	24.8	50.4	16.5
DMF	137.9	133.4	157.7	51.0	101.0	44.9
THF	164.9	145.4	140.8	60.7	177.9	61.0
1,4-Dioxane	102.0	99.5	98.5	46.5	99.4	48.2
DMAc	182.5	186.8	216.6	54.7	180.3	55.4
2094 (20% Carbon Black)						
DMSO	60.7	65.7	62.4	24.0	39.1	60.9
DMF	17.3	27.1	36.7	13.0	116.2	45.1
THF	130.6	124.2	117.2	55.8	140.4	55.8
1,4-Dioxane	85.8	85.2	84.0	43.7	84.2	42.0
DMAc	148.5	152.2	182.1	49.6	138.7	66.3
2095 (30% Carbon Black)						
DMSO	64.4	65.1	64.5	29.0	46.4	17.2
DMF	93.5	99.8	121.8	42.0	76.1	35.2
THF	117.0	102.4	109.9	^a	157.4	62.2
1,4-Dioxane	76.1	74.3	72.7	38.9	73.9	40.9
DMAc	128.9	129.2	155.4	48.6	128.4	46.3

^a Experiments were not done.

2094 polymer samples, the sorption values decrease with increasing temperature. Similarly, in the case of 1,4-dioxane, the sorption values decrease with an increase in temperature for all the polymer samples. On the other hand, DMAc exhibits increasing sorption values with temperature for all the polymers and this increase is quite considerable at 60°C when compared to 25 and 44°C. In the case of DMSO and DMF, although there is a general trend of increase in sorption with temperature, the dependency is not very systematic.

A close inspection of the sorption values with the varying amounts of carbon black in the polymers reveals that with THF, 1,4-dioxane, and DMAc a decrease in sorption is observed with increasing amount of carbon black at all temperatures. However, with DMSO and DMF, no systematic dependence of sorption on the amount of carbon black is observed. Particularly, with DMF, a considerable decrease in sorption of about 17% for sample 2094 is observed when compared to the

highest value of 138% for the sample 2093 at 25°C. However, for sample 2095, the sorption extends up to a maximum of 64%. The sorption results of DMSO, DMF, and DMAc show a dependence on their sizes, that is, these results show an increase with increasing size of solvent molecules from DMSO to DMAc via DMF. However, between THF and 1,4-dioxane, although the latter has a higher molar volume than the former, it exhibits lower sorption values at all the temperatures. This may be due to the higher polarity of THF ($\mu = 1.75$) than 1,4-dioxane ($\mu = 0.45$) although their solubility parameter values are almost identical (see Table II). Similarly, although the solubility parameter values of DMSO and DMF are identical, their sorption values are different, that is, sorption is higher for a less viscous DMF than for DMSO. Also, the viscosity of THF, being considerably smaller than 1,4-dioxane ($\eta = 1.08$ mPa s), shows increased sorption values for THF. For the majority of solvents, the desorption and redesorption data do not differ significantly. Similarly, in

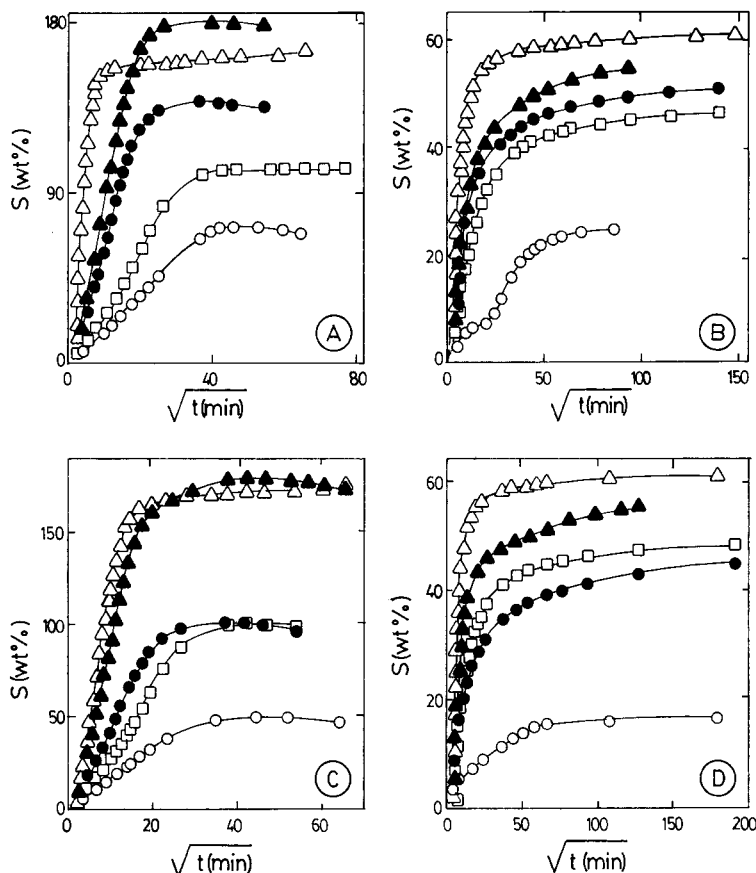


Figure 1 Plots of (A) sorption, (B) desorption, (C) resorption, and (D) redesorption results for 2093 (10% carbon black) membrane as a function of square root of time (min) at 25°C for (○) DMSO, (●) DMF, (▲) THF, (□) 1,4-dioxane, and (△) DMAc.

some cases, the sorption results at 25°C are somewhat comparable to the resorption data.

Experimental results of sorption, desorption, resorption, and redesorption for all the liquids with 2093, 2094, and 2095 polymers at 25°C are presented, respectively, in Figures 1–3. It is observed that for all the polymer–solvent systems sorption increases linearly with time in the beginning, but later reaches equilibrium. In the case of 1,4-dioxane with all the polymers, the sorption/resorption curves show more sigmoidal trends than observed for other liquids. Such sigmoidal shapes of the sorption/resorption curves with 1,4-dioxane are attributed to a smaller polarity of 1,4-dioxane ($\mu = 0.45$) as well as to its different molecular shape from other liquids, making it more difficult to enter into the available free-volume spaces of the polymer. However, this effect is not observed with the other polar liquids. In general, sorption/resorption and desorption/redesorption

curves are comparable for all the systems. In comparison to other liquids, the sorption of DMF with the 2094 membrane is extremely slow and takes a longer time than observed for other liquids. However, with the 2093 and 2095 membranes, DMSO takes quite a longer time to attain equilibrium sorption than do all the other liquids.

While studying the molecular migration of liquids into polymer membranes, diffusion has been classified as Case I (Fickian) and Case II (relaxation-controlled), that is, non-Fickian. Excellent reviews on this topic were given by Thomas and Windle,¹⁷ Frisch,¹⁸ Peterlin,¹⁹ Hansen,²⁰ and Astarita and Sarti.²¹ When liquids migrate within the network polymer, a sharp advancing concentration boundary is formed between the inner glassy portion and the outer swollen region of the polymer. The depth of the moving boundary or the sorption results could be analyzed from an empirical relationship¹¹:

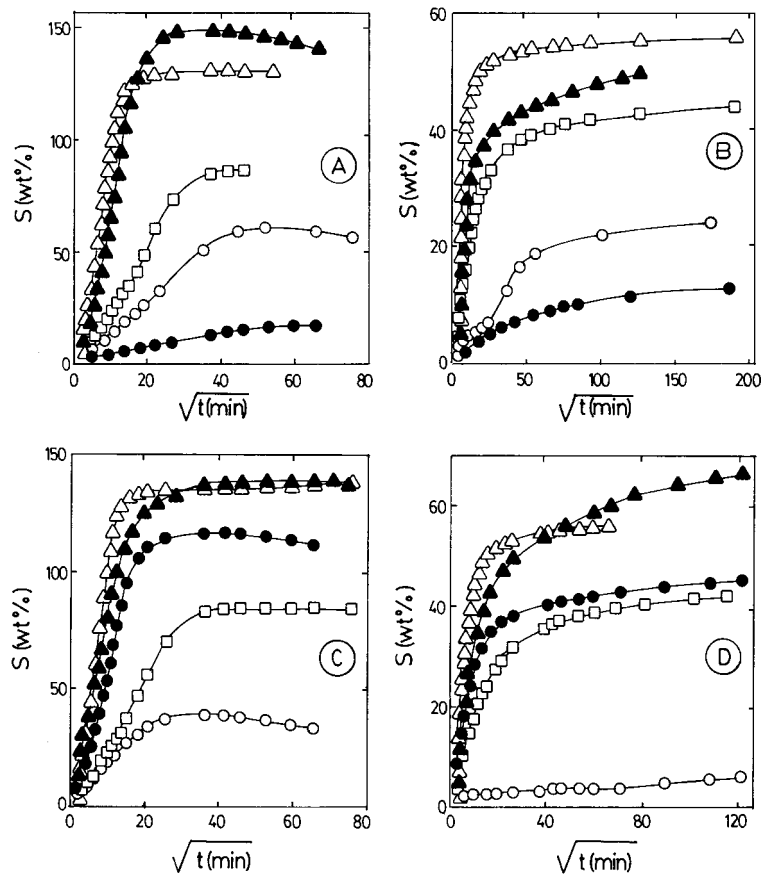


Figure 2 Plots of (A) sorption, (B) desorption, (C) resorption, and (D) redesorption results for 2094 (20% carbon black) membrane as a function of square root of time (min) at 25°C for the same liquids given in Figure 1.

$$\frac{M_t}{M_\infty} = Kt^n \quad (1)$$

where M_t and M_∞ are the values of solvent uptake (in mass percent units) at time t and at equilibrium time, and K is a parameter which depends on the nature of polymer–solvent interactions. The value of the exponent n indicates the type of transport. If the value of $n = 0.5$, then transport becomes Fickian. If $n = 1$, it is non-Fickian. On the other hand, if the values of n vary between 0.5 and 1.0, then transport is referred to as an anomalous type. Least-squares estimation of the values of K and n at 25, 44, and 60°C are given in Table IV. Values of n for all the systems range between 0.50 and 0.67, indicating an anomalous-type transport. The results of n are not affected by temperature. On the other hand, the values of K increase with temperature for all liquids in the case of the 2093 membrane, but no systematic trend is seen with

other 2094 and 2095 membranes. Also, no systematic dependence of K on the carbon black contents of the polymers is observed. Generally, smaller values of K observed for 1,4-dioxane support its lower interactions with polymer chain segments. Higher values of K observed for DMF and THF suggest their higher interactive ability with the polymer chain segments. Thus, the polarity of liquids exert an influence on the values of K .

From the sorption results, we calculated the relative concentration profiles of the liquids developed within the polymer membranes using¹¹

$$\frac{M_t}{M_\infty} = 1 - \frac{8}{\pi^2} \sum_{m=0}^{\infty} \frac{1}{(2m+1)^2} \times \exp\left[-D \frac{(2m+1)^2 \pi^2 t}{h^2}\right] \quad (2)$$

where h is the thickness of the membrane and t

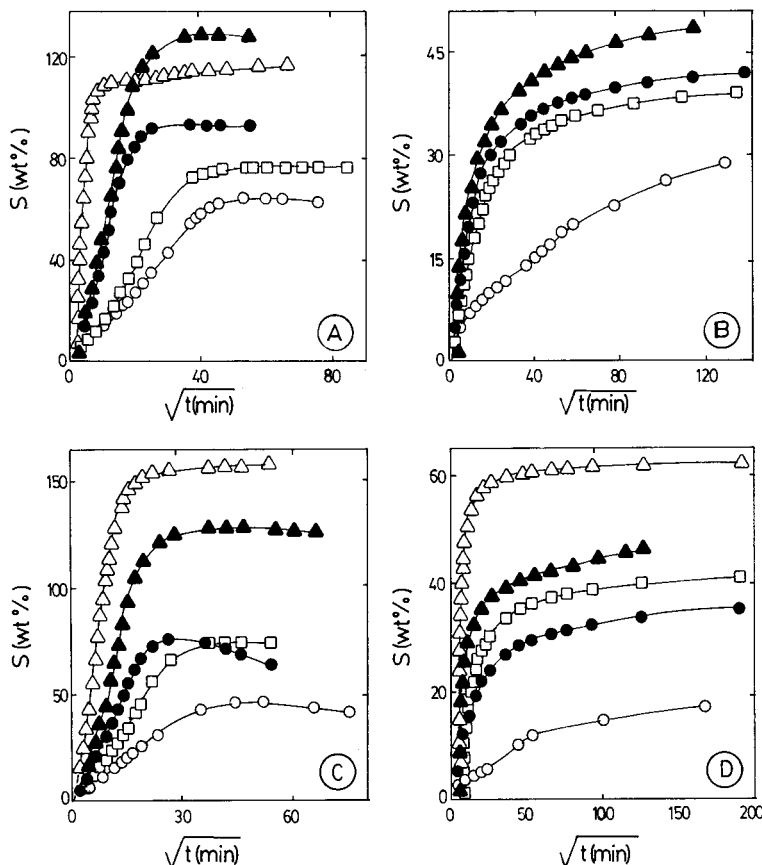


Figure 3 Plots of (A) sorption, (B) desorption, (C) resorption, and (D) redesorption results for 2095 (30% carbon black) membrane as a function of square root of time (min) at 25°C for the same liquids given in Figure 1.

is the time. Equation (2), under suitable initial and boundary conditions, is solved to give¹⁰

$$\frac{C_{(t,x)}}{C_{\infty}} = 1 - \frac{4}{\pi} \sum_{m=0}^{\infty} \frac{1}{(2m+1)} \times \exp\left[-\frac{D(2m+1)^2\pi^2t}{h^2}\right] \sin\left[\frac{(2m+1)\pi x}{h}\right] \quad (3)$$

To calculate the concentration-independent diffusion coefficients, D , we used the short-time relation¹¹:

$$\frac{M_t}{M_{\infty}} = \frac{4}{h} \left(\frac{Dt}{\pi}\right)^{1/2} \quad (4)$$

Values of D were calculated from the initial linear slopes of the plots of M_t versus $t^{1/2}$. These results are presented in Table V. Diffusion coefficients do

not exhibit any systematic dependence either on the amount of carbon black or on the size of the liquid molecules. However, the less viscous THF exhibits higher values of D at all temperatures. With the 2093 and 2095 membranes, diffusion varies according to the size of liquids and show the sequence THF > DMF > DMAc > 1,4-dioxane > DMSO. This trend is not observed for D, RS, and RD runs and also for the 2094 membrane. For all solvents, the values of D increase with increasing temperature, suggesting the creation of extra free volume within the polymer chain segments for the easy transport of liquid molecules. However, the diffusivity values for D, RS, and RD runs are different, suggesting their varying transport characteristics. Using the values of D calculated from eq. (4), theoretical sorption curves were obtained by solving eq. (2). A good agreement is seen between the solid theoretical curves and the experimental sorption points as shown in

Table IV Estimated Parameters (n and K) of Eq. (1) for the Fluoroelastomer-Liquid Systems at Different Temperatures

Liquid	n			$K \times 10^2$ (g/g min ^{n})		
	25°C	44°C	60°C	25°C	44°C	60°C
2093 (10% Carbon Black)						
DMSO	0.53	0.52	0.54	2.02	2.66	2.73
DMF	0.61	0.63	0.63	2.52	2.88	2.97
THF	0.67	0.69	0.67	3.04	3.81	4.23
1,4-Dioxane	0.58	0.58	0.59	1.61	2.21	2.58
DMAc	0.64	0.64	0.66	2.21	2.44	2.59
2094 (20% Carbon Black)						
DMSO	0.52	0.54	0.54	1.95	2.35	3.12
DMF	0.50	0.51	0.50	3.58	2.40	2.22
THF	0.67	0.67	0.67	3.28	3.92	4.58
1,4-Dioxane	0.55	0.58	0.61	1.91	2.19	2.48
DMAc	0.65	0.64	0.65	2.08	2.62	2.45
2095 (30% Carbon Black)						
DMSO	0.52	0.55	0.54	1.77	2.13	2.87
DMF	0.60	0.63	0.64	2.69	2.99	2.76
THF	0.67	0.70	0.70	2.77	3.49	3.49
1,4-Dioxane	0.57	0.58	0.60	1.51	2.14	2.42
DMAc	0.64	0.65	0.66	1.72	2.63	2.46

Figure 4 for the 2093 membrane with DMSO at 25 and 60°C.

The concentration profiles, $C_{(t,x)}/C_{\infty}$ calculated from eq. (3), along the thickness direction of the membranes are displayed in Figure 5 for THF and DMF with the 2094 membrane at 25°C for different time intervals. THF has a higher D ($= 1.04 \times 10^{-6}$ cm² s⁻¹) than DMF ($D = 7.5 \times 10^{-8}$ cm² s⁻¹) and, thus, the concentration profiles of THF reach equilibrium much faster than does DMF as shown in Figure 5. At time $t = 80$ min, THF exhibits a value of 86% for M_t/M_{∞} , whereas DMF shows a value of 70%. It may further be noted that DMF takes a longer time to reach equilibrium than does THF. In a similar manner, an increase in temperature increases diffusivity and thereby exhibits higher values of the concentration profiles (these data are not displayed to avoid redundancy).

Liquid concentration profiles have also been calculated using a numerical scheme based on the finite difference method¹⁰:

$$CN_m = \frac{1}{M} [C_{m-1} + (M - 2)C_m + C_{m+1}] \quad (5)$$

where the dimensionless parameter, M , is given as

$$M = \frac{(\Delta x)^2}{\Delta t} \frac{1}{D} \quad (6)$$

Figure 6 displays the concentration profiles obtained from this procedure for the 2094 membrane with THF and DMF at 25°C for the exposure time of 80 min. A comparison of the plots given in Figures 5 and 6 suggests that the values of the concentration profiles calculated from eq. (5) are smaller than those calculated from eq. (3), but the nature of the variations of the curves remains almost identical by both calculations.

In the present study, the results of D increase with increasing temperature. This prompted us to calculate the activation energy, E_D , for diffusion using the Arrhenius relationship:

Table V Diffusion Coefficients ($D \times 10^{-7}$, $\text{cm}^2 \text{s}^{-1}$) of Liquids with Fluoroelastomers for Sorption (S), Desorption (D), Resorption (RS), and Redesorption (RD) Runs at Different Temperatures

Liquid	S			25°C		
	25°C	44°C	60°C	D	RS	RD
2093 (10% Carbon Black)						
DMSO	0.99	1.52	2.47	0.41	2.35	0.73
DMF	3.95	6.12	6.29	11.98	3.52	4.72
THF	8.11	13.81	15.02	38.44	9.89	42.03
1,4-Dioxane	1.25	2.34	3.67	5.89	1.75	5.38
DMAc	3.55	5.03	5.91	14.53	5.57	18.37
2094 (20% Carbon Black)						
DMSO	0.94	1.68	2.43	0.36	4.45	0.14
DMF	0.75	1.15	1.22	0.36	5.11	21.15
THF	10.45	13.50	16.48	36.02	9.93	44.02
1,4-Dioxane	1.35	2.32	3.93	5.07	1.46	5.16
DMAc	3.79	5.32	5.47	14.79	7.67	11.35
2095 (30% Carbon Black)						
DMSO	0.81	1.79	2.37	0.36	1.62	0.18
DMF	3.85	6.12	6.27	9.06	3.51	3.33
THF	8.36	13.82	14.04	^a	12.28	47.35
1,4-Dioxane	1.12	2.09	3.65	4.22	1.73	4.44
DMAc	3.36	5.77	6.44	11.46	4.91	16.37

^a Experiments were not done.

$$D = D_0 \exp(-E_D/RT) \quad (7)$$

where D_0 is a constant term and RT has the conventional meaning. A representative plot of the dependence of $\log D$ on $1/T$ is displayed in Figure

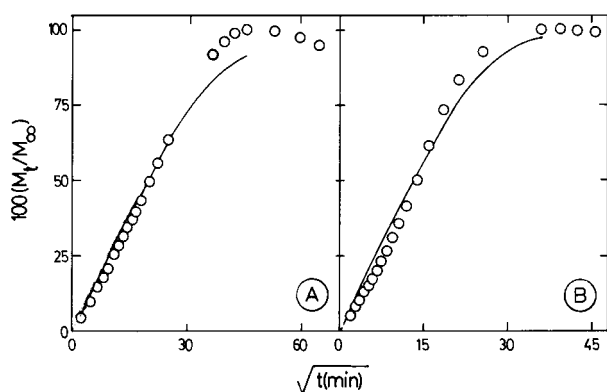


Figure 4 Comparison of the theoretical solid sorption curves calculated using eq. (2) with the experimental points for 2093 membrane with DMSO at (A) 30°C and (B) 60°C.

7. Values of E_D were calculated by the method of least-squares by fitting the $\log D$ results with $1/T$ and these data along with the estimated errors

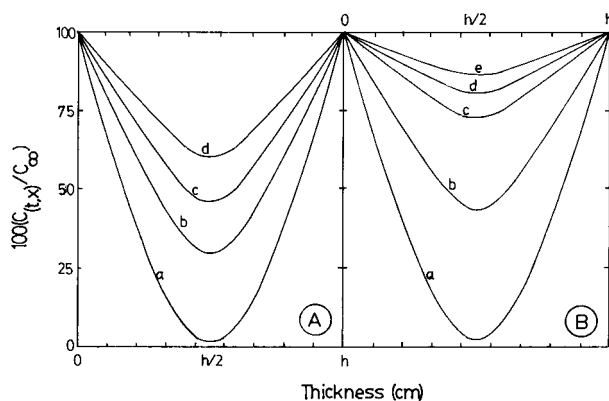


Figure 5 Dependence of concentration profiles on the thickness of polymer membranes calculated from eq. (3) for 2094 membrane (A) with DMF at time intervals of (a) 5 min, (b) 20 min, (c) 40 min, and (d) 80 min; (B) with THF at time intervals of (a) 0.6 min, (b) 4 min, (c) 20 min, (d) 40 min, and (e) 80 min at 25°C.

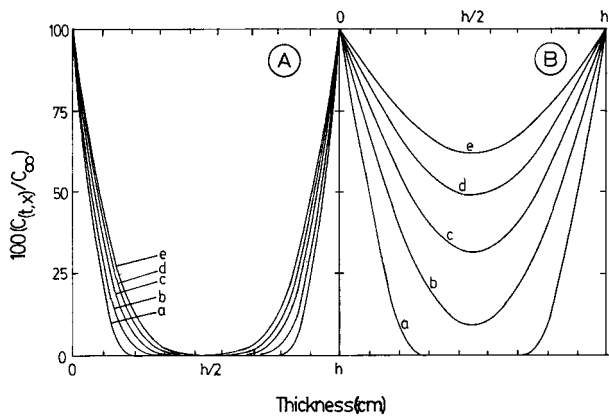


Figure 6 Dependence of concentration profiles on the thickness of polymer membranes calculated from eq. (5) for 2094 membrane: (A) with DMF and (B) THF at time intervals of (a) 4 min, (b) 20 min, (c) 40 min, (d) 60 min, and (e) 80 min at 25°C.

are presented in Table VI. It is found that for DMF having the lowest value of D with the 2094 membrane the E_D is higher than that observed for other liquids. However, for the majority of liquids, E_D values fall in the range 8.21–27.87 kJ mol⁻¹ and this range is expected of the rubbery polymer–organic liquid systems.

CONCLUSIONS

Experimental results of sorption, desorption, resorption, redesorption, diffusion, and permeation of five organic liquids with the three fluoroelastomer membranes embedded with 10, 20, and 30% of carbon blacks are presented at 25, 44, and 60°C. It is observed that both the sorption and permeation results are affected by the amount of carbon black in the polymers and these results decrease with an increasing amount of carbon black for DMSO, 1,4-dioxane, and DMAc. The lower diffusive and permeability trends are observed for samples containing higher amounts of carbon black and vice versa. From the S–D–RS–RD testing of the chosen polymer–solvent systems, it is found that the sorption and resorption results are somewhat identical. Similarly, the results of desorption and redesorption are identical. However, the cyclic S–D–RS–RD testing of the polymers does not give any quantitative clue about the morphological changes in the elastomer samples. Sorption/desorption results were analyzed by

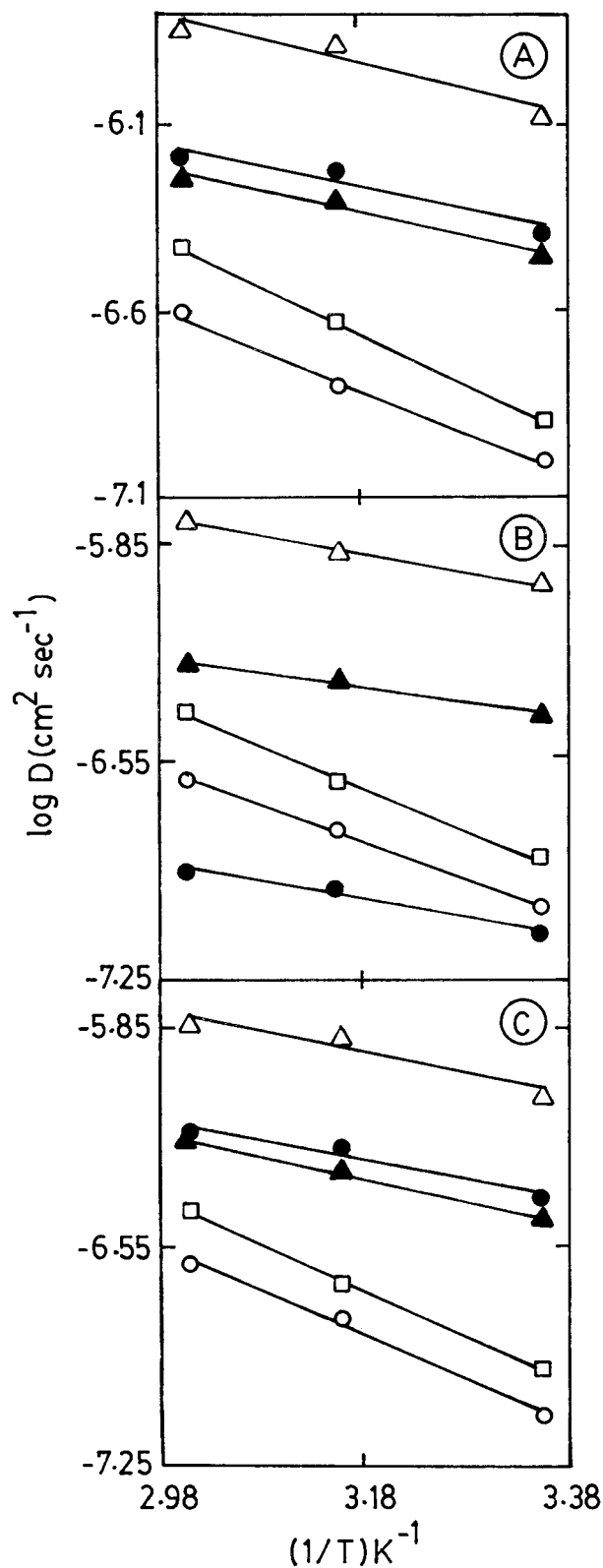


Figure 7 Arrhenius plots of $\log D$ versus $1/T$ for (A) 2093, (B) 2094, and (C) 2095 membranes with the same liquids given in Figure 1.

Table VI Activation Energy for Diffusion (E_D) (kJ mol^{-1}) of Liquids with Fluoroelastomers

Liquid	2093 (10% Carbon Black)	2094 (20% Carbon Black)	2095 (30% Carbon Black)
DMSO	21.38 (± 2.46)	22.58 (± 1.14)	25.78 (± 4.89)
DMF	11.34 (± 4.66)	11.99 (± 4.07)	11.90 (± 5.04)
THF	14.94 (± 4.87)	10.74 (± 0.10)	12.68 (± 5.60)
1,4-Dioxane	25.39 (± 0.39)	25.08 (± 1.79)	27.87 (± 1.34)
DMAc	12.16 (± 1.57)	8.95 (± 3.54)	15.75 (± 4.61)

Fick's equation and also a numerical scheme based on the finite difference method.

The authors are thankful to the All India Council for Technical Education, New Delhi [Grant No. 8017/RDII/96 (ID No. 138.23)] for a major financial support of this study.

REFERENCES

1. E. Ruckenstein and L. Liang, *J. Membr. Sci.*, **110**, 99 (1996).
2. T. M. Aminabhavi, R. S. Khinnavar, S. B. Harogopad, U. S. Aithal, Q. T. Nguyen, and K. C. Hansen, *J. Macromol. Sci. Rev. Macromol. Chem. Phys. C*, **34**, 139 (1994).
3. B. B. Gupta, A. Chaibi, and M. Y. Jaffrin, *Sep. Sci. Technol.*, **30**, 53 (1995).
4. S. Sourirajan, *Reverse Osmosis*, New York: Academic Press, (1970).
5. D. Mukherjee, A. Kulkarni, A. Chawla, and W. N. Gill, *Chem. Eng. Commun.*, **130**, 127 (1994).
6. E. M. Dannenberg, *Ind. Eng. Chem.*, **40**, 2199 (1948).
7. B. B. S. T. Boonstra and E. M. Dannenberg, *Rubb. Age* **82**, 838 (1958).
8. L. S. Waksman, N. S. Schneider, and N. H. Sung, *Barrier Polymers and Structures*, ACS Symposium Series 423, W. J. Koros, Ed., Washington, DC, 1990, Chap. 20.
9. E. Von Meerwall and R. D. Ferguson, *J. Appl. Polym. Sci.*, **23**, 3657 (1979).
10. J. M. Vergnaud, *Liquid Transport Processes in Polymeric Materials. Modeling and Industrial Applications*, Prentice-Hall, Englewood Cliffs, NJ, 1991.
11. J. Crank, *The Mathematics of Diffusion*, 2nd ed., Oxford, Clarendon, 1975.
12. M. Zinbo and A. N. Theodore, *Ind. Eng. Chem. Res.*, **33**, 1017 (1994).
13. R. G. Arnold, A. L. Barney, and D. C. Thompson, *Rubb. Chem. Technol.*, **46**, 619 (1973).
14. T. M. Aminabhavi, H. T. S. Phayde, and J. D. Ortego, *J. Hazardous Mat.*, **46**, 71 (1996).
15. T. M. Aminabhavi, H. T. S. Phayde, and J. D. Ortego, *Polym. Polym. Compos.*, **4**, 13 (1996).
16. T. M. Aminabhavi, H. T. S. Phayde, and J. D. Ortego, *Polym. Polym. Compos.*, **4**, 103 (1996).
17. N. L. Thomas and A. H. Windle, *Polymer*, **21**, 613 (1980).
18. H. L. Frisch, *Polym. Eng. Sci.*, **20**, 2 (1980).
19. A. Peterlin, *Polym. Eng. Sci.*, **20**, 238 (1980).
20. M. C. Hansen, *Polym. Eng. Sci.*, **20**, 252 (1980).
21. G. Astarita and G. C. Sarti, *Polym. Eng. Sci.*, **18**, 388 (1980).